HHS Public Access

Author manuscript

J Surg Oncol. Author manuscript; available in PMC 2021 December 01.

Published in final edited form as:

J Surg Oncol. 2020 December ; 122(8): 1711–1720. doi:10.1002/jso.26190.

Dual-agent fluorescent labelling of soft-tissue sarcomas improves the contrast based upon targeting both interstitial and cellular components of the tumor milieu

Hira Shahzad Sardar[1], **Qais Zai**[2], **Xiaochun Xu**[3], **Jason R. Gunn**[1], **Brian W. Pogue**[1,3], **Keith D. Paulsen**[1,3], **Eric R. Henderson**[1,2,4], **Kimberley S. Samkoe**[1,2,3]

[1]Thayer School of Engineering, Dartmouth College, Hanover, NH 03755

[2]Geisel School of Medicine, Dartmouth College, Hanover, NH 03755

[3]Department of Surgery, Dartmouth-Hitchcock Medical Center, Lebanon, NH 03756

[4]Department of Orthopaedics, Dartmouth-Hitchcock Medical Center, Lebanon, NH 03756

Abstract

Background: Current practices for fluorescence guided surgery utilize a single fluorescent agent, but homogeneous distribution throughout the tumor is difficult to achieve. We hypothesize that administering a perfusion and a molecular-targeted agent at their optimal administration-to-imaging time would improve whole-tumor contrast.

Experimental Design: Mice bearing subcutaneous xenograft human synovial sarcomas were administered indocyanine green (3 mg/kg) or ABY-029 (48.7 μg/kg) – an epidermal growth factor receptor targeted Affibody molecule – alone or in combination. Fluorescence contrast and signal distribution was compared between treatment groups. Two commercial fluorescence imaging systems were tested for simultaneous imaging of ICG and ABY-029.

Results: ABY-029 has a moderate positive correlation with viable tumor ($\rho = 0.2 \pm 0.4$), while indocyanine green (ICG) demonstrated a strong negative correlation ($\rho = -0.6 \pm 0.1$). Contrast-to-variance ratio was highest in the ABY-029+ICG (2.5±0.8), compared to animals that received ABY-029 (2.3±0.8) or ICG (2.0±0.5) alone. Moreover, the combination of ABY-029+ICG minimizes the correlation between viable tumor and fluorescence intensity ($\rho = -0.1 \pm 0.2$) indicating the fluorescence signal distribution is more homogeneous throughout the tumor milieu.

Conclusion: Dual-agent imaging utilizing a single channel in commercial fluorescence guided imaging system tailored for IRDye 800CW is a promising method to increase tumor contrast in a clinical setting.

Introduction

Surgical resection remains the primary treatment for many solid neoplasms. Curative surgical management of non-metastatic soft-tissue sarcomas generally requires the cancer be

Corresponding Author: Kimberley S. Samkoe, PhD; Department of Surgery; One Medical Center Drive; Lebanon, NH 03756; kimberley.s.samkoe@dartmouth.edu; Phone: +1-603-650-7618.

removed with a zone of normal tissue surrounding it, termed a wide local excision (WLE). A successful WLE therefore requires the surgeon to dissect around the tumor without direct visualization of the mass itself. Surgeons who perform WLEs therefore rely on cross-sectional radiological imaging, anatomical landmarks, tactile feedback, and conventional white light imaging.

Fluorescence-guided surgery (FGS) is a nascent technology that aims to label important tissues with fluorescent reporters (fluorophores) to improve intraoperative identification. Fluorophore tissue-labeling strategies include non-specific intravascular reporters, molecular-targeted reporters, and activatable reporters. FGS applications have focused primarily on cancer surgery with notable improvements in outcomes, particularly for glioma surgery [1]. Our team has developed an epidermal growth factor receptor (EGFR) targeted Affibody molecule® (Affibody AB) labeled with IRDye 800CW (LI-COR Biosciences) that is currently in an on-going first-in-human Phase 0 trial (NCT0315411) for soft-tissue sarcomas [16]. Pre-clinically, we have demonstrated in xenograft murine models of soft-tissue sarcoma that ABY-029 was retained longer within tumor tissue and achieved higher tumor contrast as compared to a non-specific perfusion dye (IRDye 700DX carboxylate) administered at the same concentration [15]. Interestingly, in this study we observed heterogeneous localization of ABY-029 with reduced contrast in regions of tumor necrosis. This same observation has been qualitatively noted in the human clinical trial, with a representative example shown in Figure 1. Comparatively, the perfusion dye in the pre-clinical study appeared to pool within the interstitial and necrotic spaces. However, ABY-029 and IRDye 700DX are imaged in separate fluorescence channels in commercial imaging systems due to the ~100 nm separation of their emission peak maxima.

Indocyanine green (ICG) is a longstanding, untargeted intravascular probe with FDA approval that has historically been used to facilitate intraoperative perfusion mapping [2]. More recently, ICG imaging that is performed 24-hours after administration, or during its “second window”, has proven useful in multiple cancer-centered clinical trials by exploiting the enhanced permeability and retention (EPR) effect [3, 17–21]. Unlike molecular targeted agents, ICG and other perfusion agents collect in the interstitial spaces of the tumor and fluorescence contrast arises from the differential of tissue clearance rather than differences in molecular expression. In addition, ICG has been found to localize in necrotic regions of normal tissue through association with lipoproteins and phosphoproteins. This FGS technique provides improved contrast for longer periods compared to traditional ICG angiography and has been demonstrated in soft-tissue sarcoma [4]. In addition to its clinical relevance, ICG has a larger spectral overlap with ABY-029 than IRDye 700DX, with only ~15–35 nm separation of fluorescence emission maxima depending on environment. Therefore, ICG and ABY-029 can be imaged in the same near-infrared (NIR) fluorescence channel of many commercial systems. The goal of this investigation was to determine if co-administration of ICG and ABY-029 in human soft-tissue sarcoma xenografts would produce higher contrast than single-agent administration. We hypothesized that dual-agent fluorophore administration would result in higher overall tumor contrast.

Materials and Methods

Imaging Agents

Chem Impex International powdered indocyanine green (3 mg/kg) was prepared in purified water and was intravenously injected into the tail vein of each mouse 24 hours prior to sacrifice (n=10) [4]. Stock solutions of Good Laboratory Practices (GLP) produced ABY-029 (0.42 mg/ml) were diluted to 4.98 μM with phosphate buffered saline (PBS) for administration [5]. This concentration is the mouse equivalent to the 6X human microdose of ABY-029. ABY-029 was administered via tail vein injection 4 hours prior to sacrifice (48.7 μg/kg, n=10). For mice receiving both ICG and ABY-029 (n=10), the agents were administered to the same mouse 24 and then 4 hours prior to sacrifice for ICG and ABY-029, respectively. Mouse-equivalent doses were converted from human and dog [4] using the methods of Reagan-Shaw et al [6]. One mouse in the ICG+ABY-029 group died during anesthesia and was excluded from the study.

Animal experimentation

Cell line and culture methods—The human tumor cell line SW-982 (synovial sarcoma) was obtained from ATCC (Manassas, VA, USA) and cultured as according to ATCC specifications.

Tumor implantation—All animals were used according to the guidelines approved by the Institutional Animal Care and Use Committee at Dartmouth College. Tumors were implanted subcutaneously in the right flank of 30 NSG (Jackson Laboratory, Ellsworth, ME) mice at a density of 1×10^6 cells in 200 μL in a 1:1 mixture of culture medium and Matrigel®. One of the mice from the ABY-029 only category died during injection. Therefore, a total of 29 mice were analyzed. The tumors were excised when tumor volume was approximately ~1,500 mm^3.

Imaging protocols—The mice were anesthetized (1–2.5% isoflurane, 1L/min O_2) prior to sacrifice (24 hours and 4 hours post ICG and/or ABY-029 administration, respectively. The tumors and normal surrounding tissues were exposed by surgically removing the skin from the hind leg. Each mouse was first imaged using the 750 nm channel on Solaris (Perkin Elmer) and then using SPY Elite (Novadaq) in vivo with a black cloth covering unimaged portions of the mouse to limit fluorescence signal from the abdominal organs. After imaging, the tumors were removed leaving as much normal surrounding tissue as possible for margin assessment. The tumor was then cut to reveal the normal tissue margins for the six sides and imaged on the Odyssey CLx (LI-COR Biosciences, Inc.) at 42 μm resolution. The imaging parameters used are the same as mentioned in [5].

Pathology—Tissue sections from each mouse were fixed in 10% buffered formalin (Biochemical Science, Inc.) in histological cassettes. Standard H&E was performed on all tissues. Images of the H&E sections were collected on an Olympus BX50 scope at 4x magnification.

Image Analysis—The H&E images and the Odyssey fluorescence images were aligned using the Align image by line ROI plugin in FIJI [7]. During handling of tissue, some tissues broke, others had shrunk, making the alignment difficult; therefore, the tissue images that had been significantly modified from the fresh tissue were excluded. A total of 54 of 117 images were used for the final investigation: 15 for ABY-029 category, 21 for ICG category and 18 for ABY-029+ICG category. Once the H&E image was aligned to the fluorescence image, we deconvolved the image into violet, red and green using the H&E vector in Color Deconvolution plugin. The violet image was used to calculate the intensity of viable tumor in a given ROI, where viable tumor cells are represented by the combined hematoxylin (nuclei, blue) and eosin (protein, pink) stains. Interstitial spaces, including necrotic and acellular regions, within the tumor all appear pink due to the lack of nuclei.

Phantom experimentation

The preparation of the gelatin phantoms and analysis techniques have been well described earlier [5]. Briefly, gelatin (10% w/v) was mixed with boiling distilled water, stirred vigorously while cooling to ~30°C when blood and intralipid were added according to the type of the tissue being made. Wedge phantoms were used to determine the effect of tumor and tissue properties on depth of imaging. Surgical phantoms were used to: 1) determine the effect of tissue volume on observed fluorescence; 2) to determine fluorescence intensity target values for a tumor-mimicking inclusion with a 1-cm margin, and 3) a blinded surgical phantom dissection using the fluorescence intensity target values to dissect inclusion with 1-cm margins.

Results

Specificity of ABY-029 and ICG in mouse model ex vivo

The fluorescence distribution of ABY-029 and ICG are compared in Figure 2. The variation in violet color intensity, representative of viable tumor cells, in H&E (Figures 2a and 2b) and the corresponding fluorescence intensity (Figures 2c and 2d) for a representative sarcoma injected with ABY-029 and ICG, respectively. These two mice were chosen at random and represent the average trends seen in all of the mice of a particular category. A corresponding line region-of-interest (yellow) was drawn on both the H&E and fluorescence images using FIJI, and the resulting line plots are shown (Figures 2e and 2f). For ABY-029, the violet intensity (viable tumor) and the fluorescence intensity demonstrate direct correlation. For ICG, violet and fluorescence intensities are inversely proportional. In Figures 2g and 2h, the violet intensity is plotted compared to ABY-029 and ICG fluorescence intensities, respectively, and Spearman's correlation coefficient is determined. The average Spearman's correlation coefficient (SCC) was 0.22 ± 0.4 for mice receiving ABY-029 alone; SCC was -0.63 ± 0.1 for mice receiving ICG alone.

Sensitivity of IRDye 800CW and ICG in phantoms using open air fluorescence systems

The supplemental data depicts the depth of imaging (DOI) for various wedge phantom configurations. DOI is lower for SPY than Solaris for IRDye 800CW, the fluorescent part of ABY-029, and ICG. DOI was greater for fat-simulating phantoms compared to muscle-simulating phantoms. As seen in Tables S1 and S2, DOI increases proportionately with the

diameter of the cylindrical inclusion and concentration of the agent in the inclusion. Table S3 demonstrates that DOI is inversely proportional to both intralipid and blood concentration. Here, intralipid acts as a scattering agent and blood as an absorbing agent. It must be noted that we could not detect IRDye 800CW in most configurations of the gelatin phantoms using SPY Elite.

The surgical testing phantoms were used to evaluate the target fluorescence values on both systems that correspond to a margin of 1 cm. Using these values, a surgeon blinded to the location of the inclusion successfully dissected all surgical phantoms using Solaris but was unsuccessful at four surgical phantoms when using SPY Elite. Figure 3 shows the average fluorescence values and the corresponding margins. The average fluorescence intensity increased with increasing background fluorescence. It was determined based on sensitivity, depth of imaging, and surgical accuracy that the Solaris system outperformed the SPY Elite for both IRDye 800CW and ICG.

Tumor visualization using multiple agents in mouse model in vivo

Using the Solaris as the optimal FGS system, the imaging sensitivity of tumor visualization using multiple agent imaging in vivo was investigated. Figure 4a shows example Solaris images for mice from all three categories: mice injected with ABY-029 only, with ICG only and with ABY-029 and ICG. Figure 4b depicts the average fluorescence seen on Solaris in both tumor and normal tissue in all three categories of mice. The highest fluorescence is observed when a combination of ABY-029 and ICG is used. Figure 4c presents the signal to noise ratio (SNR), tumor to background ratio (TBR) and the contrast variability ratio (CVR), each defined as:

$$SNR = \frac{\mu(I_{TUM})}{\sigma(I_{NORM})} \tag{1}$$

$$TBR = \frac{\mu(I_{TUM})}{\mu(I_{NORM})} \tag{2}$$

$$CVR = \frac{\mu(I_{TUM}) - \mu(I_{NORM})}{\sqrt{\sigma(I_{TUM})^2 - \sigma(I_{NORM})^2}} \tag{3}$$

When using dual-agent imaging (ABY-029 + ICG) the SNR increased by 78.4% as compared to ABY-029 only and by 66.0% compared to ICG only (Fig. 4). The TBR increased by 57.6% as compared to ABY-029 alone and decreased by 5.04% compared to ICG alone. The CVR increased by 7.80% and 21.5% as compared to ABY-029 and ICG only, respectively. Improved tumor visualization is observed in vivo when a dual-agent imaging is implemented with a combination of ABY-029 and ICG.

Specificity of multiple agents in mouse model ex vivo

Figure 5 presents a representative example of an excised tumor from a mouse injected with a combination of ABY-029 + ICG. Figures 5a and 5b show the color deconvolved H&E and the corresponding fluorescence image, respectively. Figure 5c shows the variation in violet color (viable tumor) and fluorescence intensity along the line region of interest drawn on the H&E and fluorescent images. Unlike the tumors excised from animals injected with ABY-029 or ICG alone (Figure 2), ABY-029 + ICG does not appear to correlate well with viable tumor cells (Figure 5d). The Spearman's correlation coefficient demonstrates that ABY-029 + ICG fluorescence does not demonstrate a significant correlation to the violet color of the H&E ($\rho = -0.092 \pm 0.23$), in comparison to ABY-029 and ICG alone that are highly positive and highly negatively correlated (Figure 5e) as reported above. The combination of ABY-029 + ICG together minimizes the correlation between violet intensity and fluorescence intensity, while maximizing tumor to normal tissue contrast.

Discussion

Targeted molecular agents are being increasingly developed to enhance recognition of tumor tissue and lengthen the window of tumor labeling; thereby yielding molecular-guided surgery in the truest sense. Many of the cancers for which FGS has been developed are surface tumors, where direct visualization by the surgeon is straightforward. Many solid organ cancers, such as soft-tissue sarcomas (STS) that are derived from the bones, muscles, nerves, and fat, are typically present at a subsurface level. Resection of these subsurface tumors is performed via 'wide local excision' where a single, complete mass is removed with an intact zone of normal tissue (~ 1 cm 'margin'). At present, positive margin rates are 22% to 34% for sarcoma and it is well known that positive margins lead to tumor recurrence [8]. It is known that STSs overexpress epidermal growth factor receptor (EGFR) in 43% to 78% of the cases [9–13]. ABY-029 is a near-infrared fluorophore, developed for clinical use [16]. ABY-029, developed under Good Manufacturing Practice (GMP) production, received eIND (#122681) approval status in 2016. One of the main advantages of ABY-029 is its short plasma half-life [5] and rapid normal tissue clearance [14], which makes surgery possible only a few hours after administration. Our pre-clinical studies in xenograft STS murine models demonstrate that maximal accumulation of ABY-029 within the tumor occurs between 4–8 hours after administration and significant tumor-to-background ratios (TBR) are observed starting at 4 hours [15]. In an ongoing clinical trial (NTC03154411), we are investigating microdose (30 nanomoles) and near microdose (90 and 180 nanomoles) administration of ABY-029 as a molecular-targeted FGS imaging agent in STS patients.

In the described work, we compared the specific distribution of tumor labeling of both non-targeted ICG and targeted ABY-029 for tumor visualization ex vivo in a pre-clinical synovial sarcoma (SW982 model) xenograft murine model. Furthermore, we compared the detection sensitivity of two near-infrared (NIR) surgical imaging systems, Solaris (Perkin Elmer) and SPY Elite (Novadaq), in gelatin phantom models of sarcoma. Once we established the imaging system that best images both agents, we investigated a "dual-agent imaging" technique for tumor visualization in a single fluorescence channel using ICG and ABY-029 simultaneously at their optimal administration-to-imaging times in vivo. We then compare

the specificity of using a combination of the non-targeted agent ICG and the targeted agent ABY-029 to using either alone ex vivo. We aim to establish best practice methodology for maximal tumor and margin detection during NIR-guided surgical dissection for human STS.

The ability to visualize the entire tumor in order to excise with negative margins is essential to preventing recurrence. However, we have noted both in pre-clinical murine work [15] and the Phase 0 human trial (data not shown, representative image shown in Figure 1) that ABY-029 fails to label the tumor completely due to: 1) highly heterogeneous distribution of EGFR within viable tumor tissue, and 2) large regions of necrosis. These non-highlighting regions can lead to lower average tumor fluorescence signals and potentially lower contrast. This is especially important in soft-tissue sarcoma surgeries that are performed as a wide local excision, where indirect visualization requires high contrast in all tumor regions.

We previously compared the uptake of ABY-029, an EGFR-targeted peptide, with IRDye 700DX carboxylate, a non-specific fluorophore that acted as a perfusion agent [14]. In this study it was readily observed that the ABY-029 and IRDye 700DX were localizing to different regions of the same tumor. It appeared that IRDye 700DX was localizing to regions of low cellular density, including regions of necrosis, while ABY-029 appeared to be more evenly distributed throughout the viable tissue. However, IRDye 700DX is not readily used in clinical imaging and not comparable to other published studies. In addition, the IRDye 700DX emission maximum has ~100 nm spectral separation from ABY-029 emission maximum, making simultaneous detection difficult especially on commercially available systems. Therefore, we undertook these studies using ABY-029 and ICG, a clinically relevant, non-specific imaging agent that monitors tissue perfusion and vascular function. Unlike our previous study with IRDye 700DX where both agents could be administered in the same animal using two distinct fluorescence imaging channels, different animals had to be used for imaging each agent individually as there is significant spectral overlap in the absorption and emission spectra. A similar distribution of the targeted and untargeted agents was observed with ABY-029 localizing to more cellular regions and ICG localizing to less cellular regions (Figure 5b and 5c). This trend was verified by performing line plot analysis of viable tumor cells (purple color in H&E) and fluorescence intensity. ABY-029 had a moderate positive correlation with viable tumor ($\rho = 0.22 \pm 0.4$), while ICG had a strong negative correlation with viable tumor ($\rho = -0.63 \pm 0.1$). The clear delineation between the localization of the two imaging agents presented the hypothesis that administering both agents at the optimal administration-to-imaging window could allow a more homogeneous distribution throughout the entire tumor (Figure 6). However, both agents would have to be imaged in the same channel of surgical system due to the significant spectral overlap.

We undertook a gelatin phantom imaging study to test the sensitivity of both IRDye 800CW, the fluorescent part of ABY-029, and ICG using two open air fluorescence systems, Solaris and SPY Elite, based on experiments performed previously with IRDye 800CW alone [5]. The Solaris has two channels capable of imaging both IRDye 800CW and ICG. We used the 750 nm channel that has a 743 nm LED for excitation and emission band pass at 770 to 809 nm. In comparison, SPY Elite only has one channel with 805 nm laser excitation and 825–830 nm bandpass emission filter. These systems have performed similarly in detecting IRDye 800CW [15], although the optics of the SPY Elite are tailored specifically for ICG

perfusion imaging. Here, it was found that the Solaris was more sensitive in both depth and concentration detection using wedge phantoms representing muscle and fat with varying inclusion-to-background ratios of IRDye 800CW and ICG (see Supplemental Material). In surgical phantoms, where the surgeon was blinded to the location of the inclusion, the ICG inclusions were successfully removed with a negative margin using both the Solaris and the SPY Elite. However, IRDye 800CW inclusions were successfully dissected only using the Solaris, whereas several inclusions were cut into using the SPY Elite indicating a positive margin (see Supplemental Material). One limitation to the gelatin phantoms is that ICG degrades rapidly over time. In order to obtain equivalent fluorescence signal after the gelatin phantom had set 24 hours later, it was determined that the fluorescence of ICG decreases by a factor of 3 in 24 hours. Therefore, we tripled the concentration of ICG that was used to prepare the phantom in order to have a fair comparison of the images obtained. Additionally, the systems were tested with the dyes in the same molar ratio in order to determine the sensitivity, while the animal experiments were performed with ICG at a higher, clinically relevant concentration.

The Solaris provided the highest sensitivity for both imaging agents and was used to compare the image contrast of soft-tissue sarcoma xenograft tumors in vivo. In all cases, ABY-029 + ICG fluorescence and image contrast performed as well or better than either ABY-029 or ICG alone. We looked at 3 measures of image contrast - SNR, TBR and CVR. Although TBR is the most commonly used measure of tumor uptake in fluorescence guided surgery, it does not account for variability in the signal. In soft-tissue sarcoma, where fluorescence is highly heterogeneous, measures of contrast that account for variability in the signal is essential. The combination of ABY-029 + ICG had the most improvement on the mean of CVR, which considers both the mean of the fluorescence signal and the standard deviation of the signal in both the tumor and normal tissues. As can be seen in Figure 5, ex vivo analysis of spatial distribution of the fluorescence signal demonstrated that there was no measurable correlation between viable tumor cells (H&E purple stain) and fluorescence signal for the combination of ABY-029 + ICG ($\rho = -0.092 \pm 0.23$). This is a promising result as the spatial variability of fluorescence signal within the tumor was reduced while improving tumor-to-normal tissue contrast.

Maximizing distribution of fluorescent agent in order to more accurately discern the tumor from normal tissue has been achieved by using agents that localize to different but complementary regions of the tumor, as demonstrated in the schematic in Figure 6. This technique is further advantageous because both agents use imaging agents that can be imaged in a single fluorescent channel. There is no need for spectral separation or distinguishing the fluorescent agents from each other and commercial systems designed for imaging in the near-infrared spectral range are capable of detecting both agents. The addition of other region-specific fluorophores using IRDye 800CW, ICG, or other comparable fluorophores is possible that may further enhance tumor contrast.

Conclusion

This study compares the tumor contrast achieved using ICG and ABY-029 as independent and combined imaging agents to fluorescently label soft-tissue sarcomas. ABY-029, a

molecular-targeted agent, provides higher specificity to viable cellular regions of tumor (identified using the gold standard, H&E) than ICG, which preferentially—and synergistically—highlighted interstitial tumor regions, including acellular and necrotic regions. The paper also dwells upon the sensitivity of two commercially available near-infrared (NIR) surgical imaging systems, Solaris (Perkin Elmer) and SPY Elite (Novadaq), in gelatin phantom models of sarcoma. SPY Elite, designed especially for imaging tissue perfusion with ICG, is unable to be used with IRDye 800CW. We also introduce 'dual-agent imaging' that uses a combination of a non-targeted agent ICG and a targeted agent ABY-029 to improve tumor visualization and increase tissue fluorescence homogeneity both in vivo and ex vivo.

Supplementary Material

Refer to Web version on PubMed Central for supplementary material.

Acknowledgements

The authors would like to acknowledge funding from the National Cancer Institute (NCI) R37 CA212187 (KSS) and R03 CA219445 (ERH) for the development and implantation of this research and R01 CA167413 (KDP) the production of ABY-029. Author ERH would also like to acknowledge funding from the National Institute of Biomedical Imaging and Bioengineering K23 EB026507 for dedicated research effort.

References

1. Stummer W, Pichlmeier U, Meinel T, et al. Fluorescence-guided surgery with 5-aminolevulinic acid for resection of malignant glioma: a randomised controlled multicentre phase III trial. Lancet Oncol. 2006;7(5):392–401. doi:10.1016/S1470-2045(06)70665-9 [PubMed: 16648043]
2. Frangioni JV. In vivo near-infrared fluorescence imaging. Curr Opin Chem Biol. 2003;7(5):626–634. doi:10.1016/j.cbpa.2003.08.007 [PubMed: 14580568]
3. Zeh R, Sheikh S, Xia L, et al. The second window ICG technique demonstrates a broad plateau period for near-infrared fluorescence tumor contrast in glioblastoma. PLoS One. 2017;12(7):e0182034. Published 2017 Jul 24. doi:10.1371/journal.pone.0182034
4. Holt D, Parthasarathy AB, Okusanya O, et al. Intraoperative near-infrared fluorescence imaging and spectroscopy identifies residual tumor cells in wounds. J Biomed Opt. 2015;20(7):76002. doi:10.1117/1.JBO.20.7.076002
5. Samkoe KS, Bates BD, Tselepidakis NN, et al. Development and evaluation of a connective tissue phantom model for subsurface visualization of cancers requiring wide local excision. J Biomed Opt. 2017;22(12):1–12. doi:10.1117/1.JBO.22.12.121613
6. Reagan-Shaw S, Nihal M, Ahmad N. Dose translation from animal to human studies revisited. FASEB J. 2008;22(3):659–661. doi:10.1096/fj.07-9574LSF [PubMed: 17942826]
7. Schindelin J; Arganda-Carreras I. & Frise E. et al. (2012), "Fiji: an open-source platform for biological-image analysis", Nature methods 9(7): 676–682, PMID 22743772, doi:10.1038/nmeth.2019 [PubMed: 22743772]
8. Potter BK, Hwang PF, Forsberg JA, et al. Impact of margin status and local recurrence on soft-tissue sarcoma outcomes. J Bone Joint Surg Am. 2013;95(20):e151. doi:10.2106/JBJS.L.01149
9. Keizman D, Issakov J, Meller I, et al. Expression and significance of EGFR in malignant peripheral nerve sheath tumor [published correction appears in J Neurooncol. 2009 9;94(3):389.Meimon, Natalie [corrected to Maimon, Natalie]]. J Neurooncol. 2009;94(3):383–388. doi:10.1007/s11060-009-9862-z [PubMed: 19330289]
10. Teng HW, Wang HW, Chen WM, et al. Prevalence and prognostic influence of genomic changes of EGFR pathway markers in synovial sarcoma. J Surg Oncol. 2011;103(8):773–781. doi:10.1002/jso.21852 [PubMed: 21240992]

11. Yang JL, Gupta RD, Goldstein D, Crowe PJ. Significance of Phosphorylated Epidermal Growth Factor Receptor and Its Signal Transducers in Human Soft Tissue Sarcoma. Int J Mol Sci. 2017;18(6):1159. Published 2017 May 30. doi:10.3390/ijms18061159
12. Yang JL, Hannan MT, Russell PJ, Crowe PJ. Expression of HER1/EGFR protein in human soft tissue sarcomas. Eur J Surg Oncol. 2006;32(4):466–468. doi:10.1016/j.ejso.2006.01.012 [PubMed: 16524687]
13. Sato O, Wada T, Kawai A, et al. Expression of epidermal growth factor receptor, ERBB2 and KIT in adult soft tissue sarcomas: a clinicopathologic study of 281 cases. Cancer. 2005;103(9):1881–1890. doi:10.1002/cncr.20986 [PubMed: 15772959]
14. Samkoe KS, Sardar HS, Bates BD, et al. Preclinical imaging of epidermal growth factor receptor with ABY-029 in soft-tissue sarcoma for fluorescence-guided surgery and tumor detection. J Surg Oncol. 2019;119(8):1077–1086. doi:10.1002/jso.25468 [PubMed: 30950072]
15. DSouza AV, Lin H, Henderson ER, Samkoe KS, Pogue BW. Review of fluorescence guided surgery systems: identification of key performance capabilities beyond indocyanine green imaging. J Biomed Opt. 2016;21(8):80901. doi:10.1117/1.JBO.21.8.080901 [PubMed: 27533438]
16. Samkoe KS, Gunn JR, Marra K, et al. Toxicity and Pharmacokinetic Profile for Single-Dose Injection of ABY-029: a Fluorescent Anti-EGFR Synthetic Affibody Molecule for Human Use. Mol Imaging Biol. 2017;19(4):512–521. doi:10.1007/s11307-016-1033-y [PubMed: 27909986]
17. Newton AD, Predina JD, Nie S, Low PS, Singhal S. Intraoperative fluorescence imaging in thoracic surgery. J Surg Oncol. 2018;118(2):344–355. doi:10.1002/jso.25149 [PubMed: 30098293]
18. Cho SS, Jeon J, Buch L, et al. Intraoperative near-infrared imaging with receptor-specific versus passive delivery of fluorescent agents in pituitary adenomas. J Neurosurg. 2018;131(6):1974–1984. doi:10.3171/2018.7.JNS181642 [PubMed: 30554181]
19. Lee JYK, Pierce JT, Thawani JP, et al. Near-infrared fluorescent image-guided surgery for intracranial meningioma. J Neurosurg. 2018;128(2):380–390. doi:10.3171/2016.10.JNS161636 [PubMed: 28387632]
20. Cho SS, Zeh R, Pierce JT, Salinas R, Singhal S, Lee JYK. Comparison of Near-Infrared Imaging Camera Systems for Intracranial Tumor Detection. Mol Imaging Biol. 2018;20(2):213–220. doi:10.1007/s11307-017-1107-5 [PubMed: 28741043]
21. Starosolski Z, Bhavane R, Ghaghada KB, Vasudevan SA, Kaay A, Annapragada A. Indocyanine green fluorescence in second near-infrared (NIR-II) window. PLoS One. 2017;12(11):e0187563. Published 2017 Nov 9. doi:10.1371/journal.pone.0187563

Synopsis:

Current practice utilizes a single fluorescent agent but homogeneous distribution throughout the tumor is difficult to achieve. We hypothesize that administering a perfusion and a molecular targeted agent at their optimal administration-to-imaging time (AIT) in the same animal would improve whole-tumor contrast. Dual-agent imaging utilizing a single channel in commercial fluorescence guided imaging system tailored for IRDye 800CW rather than ICG is a promising method to increase tumor contrast in a clinical setting.

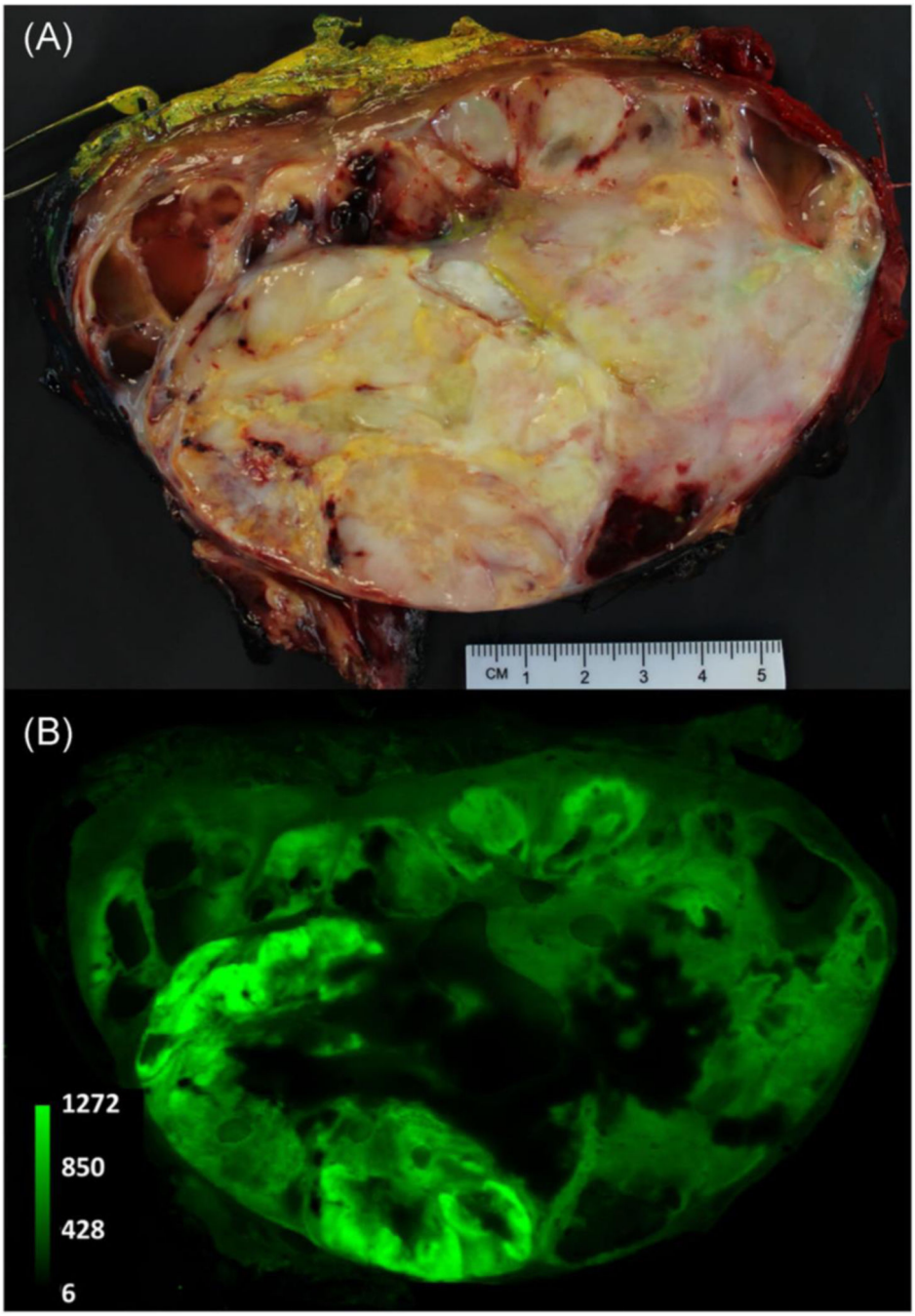

Figure 1.

A representative example of heterogeneous distribution of ABY-029 in a human soft-tissue sarcoma. The patient was administered a six-times microdose (180 nanomoles) of ABY-029 on the same day of surgery. The mass was excised via wide-local excision and a 1–2 cm thick breadloaf slice was imaged using white light photography (a) and a near-infrared fluorescence image was obtained using 800 nm channel of an Odyssey CLx (b).

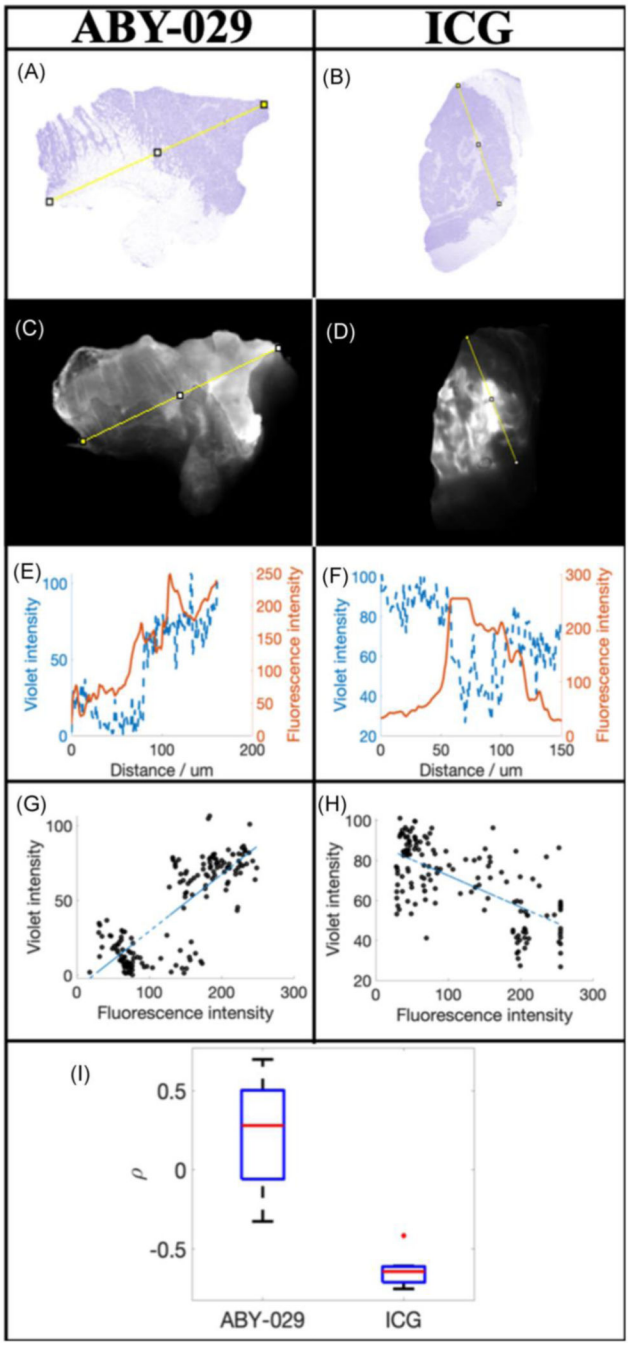

Figure 2.

Comparison of the distributions of ABY-029 and ICG in xenograft soft-tissue sarcomas. H&E (a and b) and corresponding fluorescence (c and d) images of ABY-029 and ICG, respectively. The pixel value of the violet stain and fluorescence intensity was determined along the yellow lines were plotted in (e) and (f) for ABY-029 and ICG, respectively. The Spearman's correlation coefficient between violet intensity and ABY-029 or ICG fluorescence intensity was determined from scatter plots (g and h, respectively) and the resultant coefficients plotted in (i).

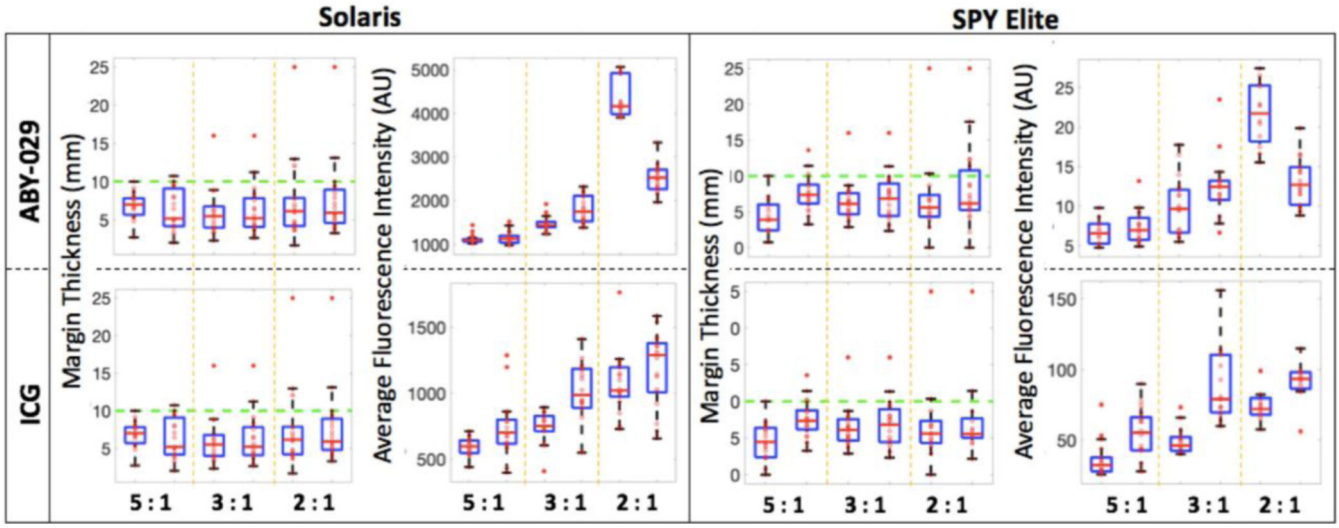

Figure 3.

Surgical phantom dissection data for ABY-029 and ICG. Margin thickness, and average fluorescence intensity from all six sides of the dissected inclusion measured both on the Solaris and the SPY Elite. The green dashed line on the margin thickness plots indicates the goal margin thickness of 10 mm.

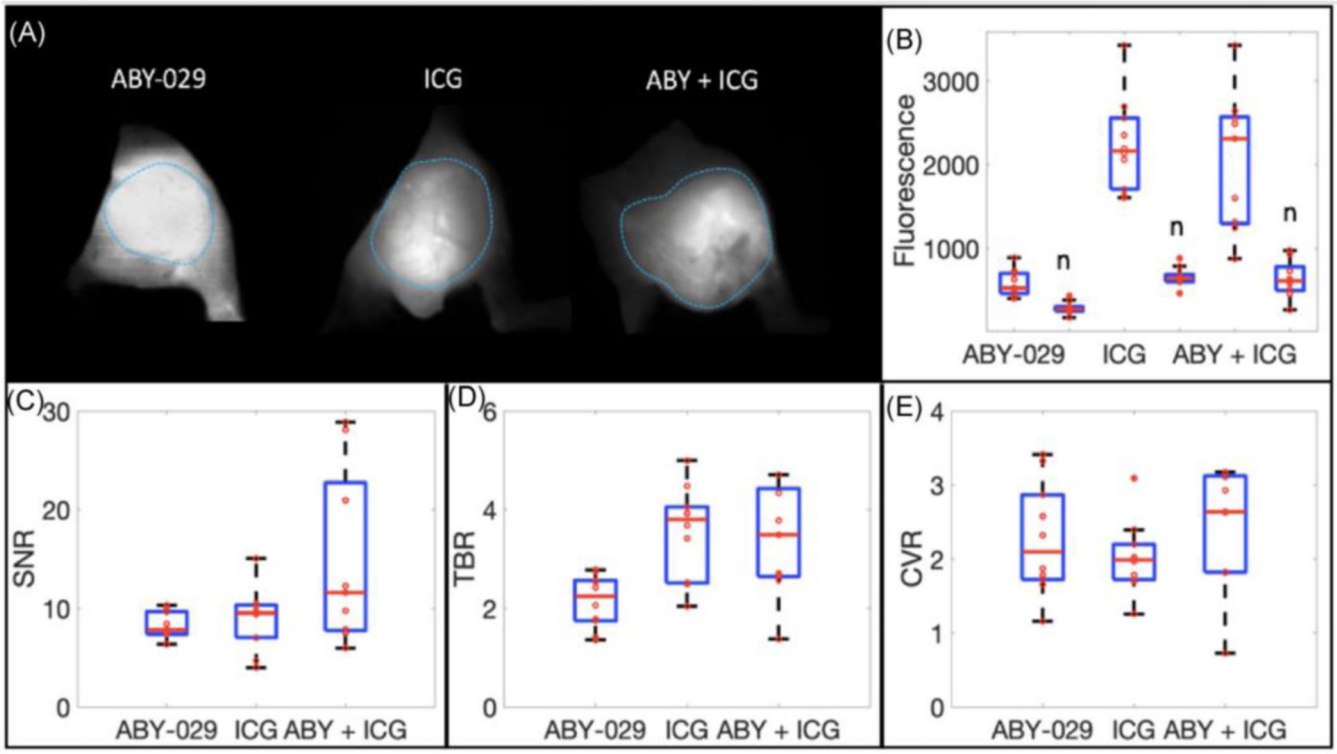

Figure 4.

In vivo fluorescence imaging of soft-tissue sarcomas. (a) Representative examples of ABY-029, ICG and ABY-029 + ICG images in murine xenograft intra-muscular tumor. (b) Average fluorescence intensities of each mouse in tumor and normal (n) tissues for each fluorophore type. Image contrast was calculated in three ways: (c) signal-to-noise ratio (SNR), (d) tumor-to-background ratio (TBR), and (e) contrast-to-variance ratio (CVR).

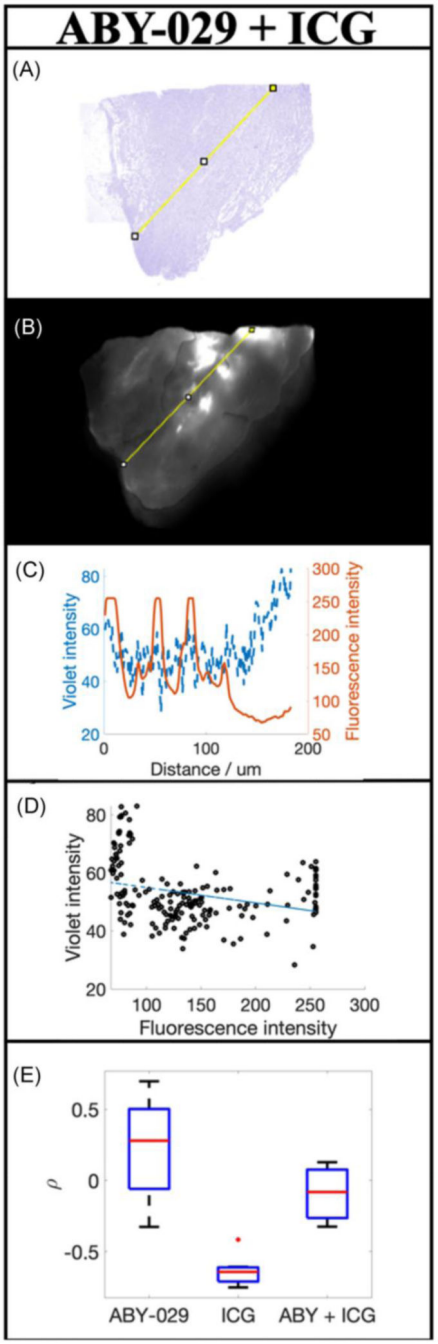

Figure 5.

The distribution of ABY-029 + ICG administered in the same animals. (a) H&E and (b) corresponding fluorescence images of ABY-029 + ICG. The pixel value of the violet stain and fluorescence intensity was determined along the yellow lines were plotted in (c) and the Spearman's correlation coefficient determined scatter plots in (d). The resultant Spearman coefficients for each animal and imaging agent type, including ABY-029 and ICG alone, are plotted in (e).

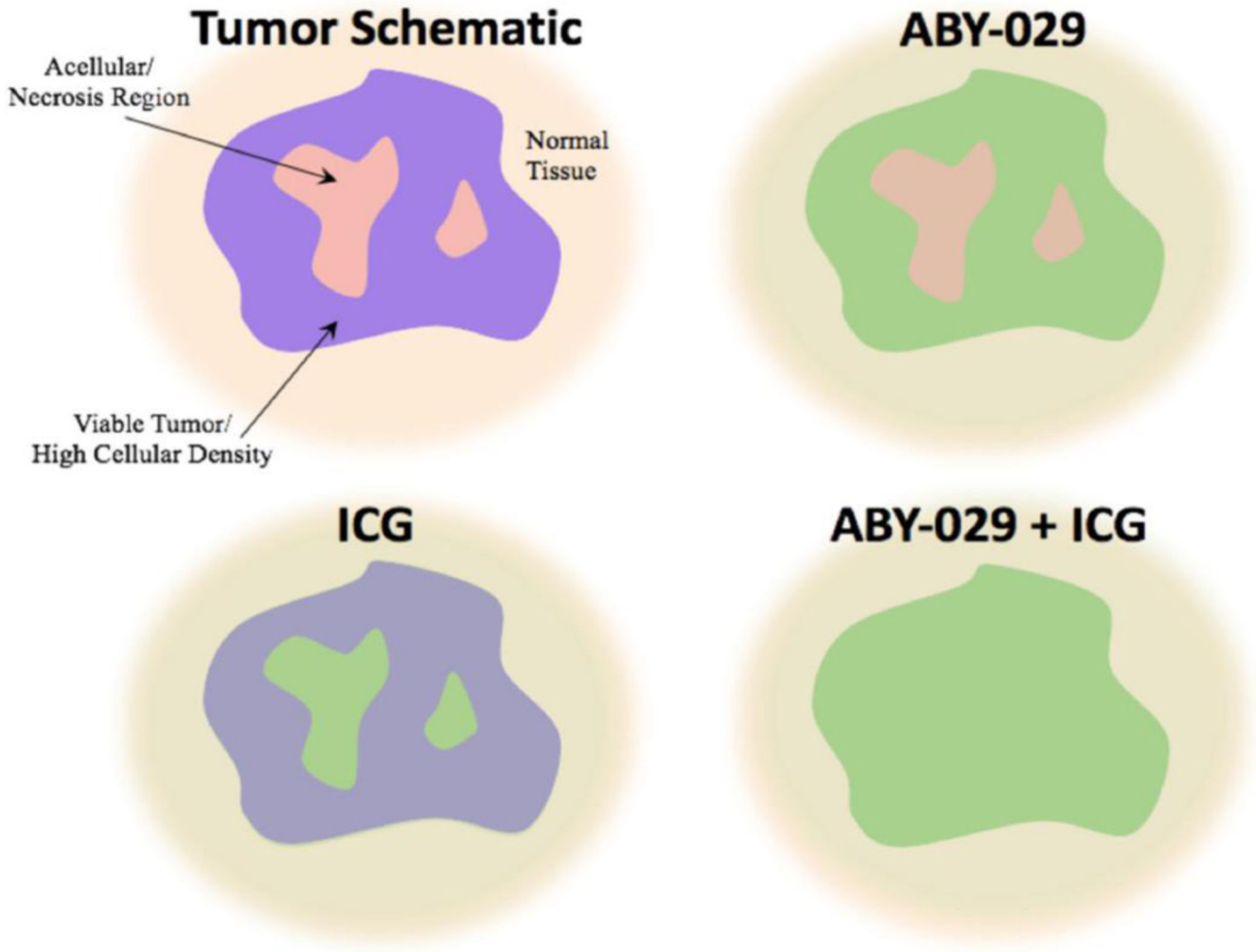

Figure 6.

The fluorescence distributions of ABY-029 alone, ICG alone, and ABY-029-ICG in a representative schematic diagram of a tumor. Viable tissue with high cellular density is indicated in violet and interstitial regions including acellular and necrotic regions are indicated by pink, as visualized in H&E. Normal surrounding tissue is given for reference. ABY-029 localizes mainly to the regions of viable tumor, where EGFR will be located, while ICG localizes more significantly to the regions of low cellular density. When combined all tissue regions have a more homogeneous distribution of fluorescence, while maintaining tumor contrast.